References

1. **Cohen LE, Radovick S** 2002 Molecular basis of combined pituitary hormone deficiencies. Endocr Rev 23:431–442
2. **Kelberman D, Rizzoti K, Lovell-Badge R, Robinson IC, Dattani MT** 2009 Genetic regulation of pituitary gland development in human and mouse. Endocr Rev 30:790–829
3. **Dateki S, Kosaka K, Hasegawa K, Tanaka H, Azuma N, Yokoya S, Muroya K, Adachi M, Tajima T, Motomura K, Kinoshita E, Moriuchi H, Sato N, Fukami M, Ogata T** 2009 Heterozygous orthodenticle homeobox 2 mutations are associated with variable pituitary phenotype. J Clin Endocrinol Metab DOI: 10.1210/jc.2009–13
4. **Coya R, Vela A, Pérez de Nanclares G, Rica I, Castaño L, Busturia MA, Martul P; GEDPIT group** 2007 Panhypopituitarism: genetic versus acquired etiological factors. J Pediatr Endocrinol Metab 20:27–36
5. **Vieira TC, Boldarine VT, Abucham J** 2007 Molecular analysis of PROP1, PIT1, HESX1, LHX3, and LHX4 shows high frequency of PROP1 mutations in patients with familial forms of combined pituitary hormone deficiency. Arq Bras Endocrinol Metabol 51:1097–1103
6. **Kim SS, Kim Y, Shin YL, Kim GH, Kim TU, Yoo HW** 2003 Clinical characteristics and molecular analysis of PIT1, PROP1, LHX3, and HESX1 in combined pituitary hormone deficiency patients with abnormal pituitary MR imaging. Horm Res 60:277–283
7. **Rainbow LA, Rees SA, Shaikh MG, Shaw NJ, Cole T, Barrett TG, Kirk JM** 2005 Mutation analysis of POUF-1, PROP-1 and HESX-1 show low frequency of mutations in children with sporadic forms of combined pituitary hormone deficiency and septo-optic dysplasia. Clin Endocrinol (Oxf) 62:163–168
8. **Abrão MG, Leite MV, Carvalho LR, Billerbeck AE, Nishi MY, Barbosa AS, Martin RM, Arnhold IJ, Mendonca BB** 2006 Combined pituitary hormone deficiency (CPHD) due to a complete PROP1 deletion. Clin Endocrinol (Oxf) 65:294–300
9. **Pfaeffle RW, Savage JJ, Hunter CS, Palme C, Ahlmann M, Kumar P, Bellone J, Schoenau E, Korsch E, Brämswig JH, Stobbe HM, Blum WF, Rhodes SJ** 2007 Four novel mutations

of the LHX3 gene cause combined pituitary hormone deficiencies with or without limited neck rotation. J Clin Endocrinol Metab 92:1909–1919

10. **Woods KS, Cundall M, Turton J, Rizotti K, Mehta A, Palmer R, Wong J, Chong WK, Al-Zyoud M, El-Ali M, Otonkoski T, Martinez-Barbera JP, Thomas PQ, Robinson IC, Lovell-Badge R, Woodward KJ, Dattani MT** 2005 Over- and underdosage of SOX3 is associated with infundibular hypoplasia and hypopituitarism. Am J Hum Genet 76:833–849
11. **Machinis K, Amselem S** 2005 Functional relationship between LHX4 and POU1F1 in light of the LHX4 mutation identified in patients with pituitary defects. J Clin Endocrinol Metab 90:5456–5462
12. **Schouten JP, McElgunn CJ, Waaijer R, Zwijnenburg D, Diepvens F, Pals G** 2002 Relative quantification of 40 nucleic acid sequences by multiplex ligation-dependent probe amplification. Nucleic Acids Res 30:e57
13. **Desviat LR, Pérez B, Ugarte M** 2006 Identification of exonic deletions in the PAH gene causing phenylketonuria by MLPA analysis. Clin Chim Acta 373:164–167
14. **Fukami M, Dateki S, Kato F, Hasegawa Y, Mochizuki H, Horikawa R, Ogata T** 2007 Identification and characterization of cryptic SHOX intragenic deletions in three Japanese patients with Léri-Weill dyschondrosteosis. J Hum Genet 53:454–459
15. **Machinis K, Pantel J, Netchine I, Léger J, Camand OJ, Sobrier ML, Dastot-Le Moal F, Duquesnoy P, Abitbol M, Czernichow P, Amselem S** 2001 Syndromic short stature in patients with a germline mutation in the LIM homeobox LHX4. Am J Hum Genet 69:961–968
16. **Tajima T, Hattori T, Nakajima T, Okuhara K, Tsubaki J, Fujieda K** 2007 A novel missense mutation (P366T) of the LHX4 gene causes severe combined pituitary hormone deficiency with pituitary hypoplasia, ectopic posterior lobe and a poorly developed sella turcica. Endocr J 54:637–641
17. **Pfaeffle RW, Hunter CS, Savage JJ, Duran-Prado M, Mullen RD, Neeb ZP, Eiholzer U, Hesse V, Haddad NG, Stobbe HM, Blum WF, Weigel JF, Rhodes SJ** 2008 Three novel missense mutations within the LHX4 gene are associated with variable pituitary hormone deficiencies. J Clin Endocrinol Metab 93:1062–1071

18. **Castinetti F, Saveanu A, Reynaud R, Quentien MH, Buffin A, Brauner R, Kaffel N, Albarel F, Guedj AM, El Kholy M, Amin M, Enjalbert A, Barlier A, Brue T** 2008 A novel dysfunctional LHX4 mutation with high phenotypical variability in patients with hypopituitarism. J Clin Endocrinol Metab 93:2790–2799

19. **Tajima T, Yorifuji T, Ishizu K, Fujieda K** 2009 A novel mutation (V101A) of the LHX4 gene in a Japanese patient with combined pituitary hormone deficiency. Exp Clin Endocrinol Diabetes DOI: 10.1055/s–0029–1225612

20. **Shaw CJ, Lupski JR** 2004 Implications of human genome architecture for rearrangement-based disorders: the genomic basis of disease. Hum Mol Genet 13:R57–R64

Figure legends

Figure 1. Gene copy number analysis.

A. MLPA and FISH analyses. The black and white boxes on genomic DNA (gDNA) denote the coding regions on exons 1–6 (E1–E6) and the untranslated regions, respectively. The sites examined by MLPA probes (A–F) are indicated by arrows, and the region identified by the 5,305-bp FISH probe is shown by a thick horizontal line. In MLPA analysis, the peaks for the sites A–F are reduced in the patient. The red peaks indicate the internal size markers. In FISH analysis, the red signal is derived from the probe for *LHX4*, and the green signals are derived from chromosome 1 centromere control probe (Cytocell, Cambridge, UK) used as an internal control. The probe for *LHX4* is labeled with digoxigenin and detected by rhodamine anti-digoxigenin, and the control probe is labeled with biotin and detected by avidin conjugated to fluorescein isothiocyanate.

B. Oligoarray CGH analysis and direct sequencing of the deletion junction. The deletion is 522,009 bp in physical size (shaded in gray) and is associated with an addition of an 8-bp segment of unknown origin (highlighted in yellow). The normal sequences flanking the microdeletion are indicated with dashed underlines.

TABLE 1. Blood hormone values of the patient with *LHX4* deletion.

Age at examination		1 yr 6 months		11 yr	
	Stimulus (dosage)	Baseline	Peak	Baseline	Peak
GH (ng/ml)	GHRH (1 μg/kg)	0.2	**1.2**		
	Arginine (0.5 g/kg)	0.1	**0.2**		
	L-Dopa (10 mg/kg)	0.1	**0.1**		
LH (mIU/ml)	GnRH (100 μg/m^2)	<0.5		0.3	**0.8**
FSH (mIU/ml)	GnRH (100 μg/m^2)	0.5		1.3	**1.6**
TSH (μU/ml)	TRH (10 μg/kg)	2.3	**3.9**		
Prolactin (ng/ml)	TRH (10 μg/kg)	**<1.0**	**<1.0**		
ACTH (pg/ml)		24.6			
Cortisol (μg/dl)[a]		17.5			
IGF-I (ng/ml)		**9**			
Free T4 (ng/dl)		**0.6**[b]			
Estradiol (pg/ml)				**<15**	

The conversion factor to the SI unit: GH 1.0 (μg/liter), LH 1.0 (IU/liter), FSH 1.0 (IU/liter), TSH 1.0 (mIU/liter), prolactin 1.0 (μg /liter), ACTH 0.22 (pmol/liter), cortisol 27.59 (nmol/liter), IGF-I 0.131 (nmol/liter), free T4 12.87 (pmol/liter), and estradiol 3.671 (pmol/liter).

Hormone values have been evaluated by the age-and sex-matched Japanese reference data; low hormone data are boldfaced.

Blood sampling during the provocation tests: 0, 30, 60, 90, and 120 minutes.

[a] Obtained at 0800h.

[b] Measured at one month of age.

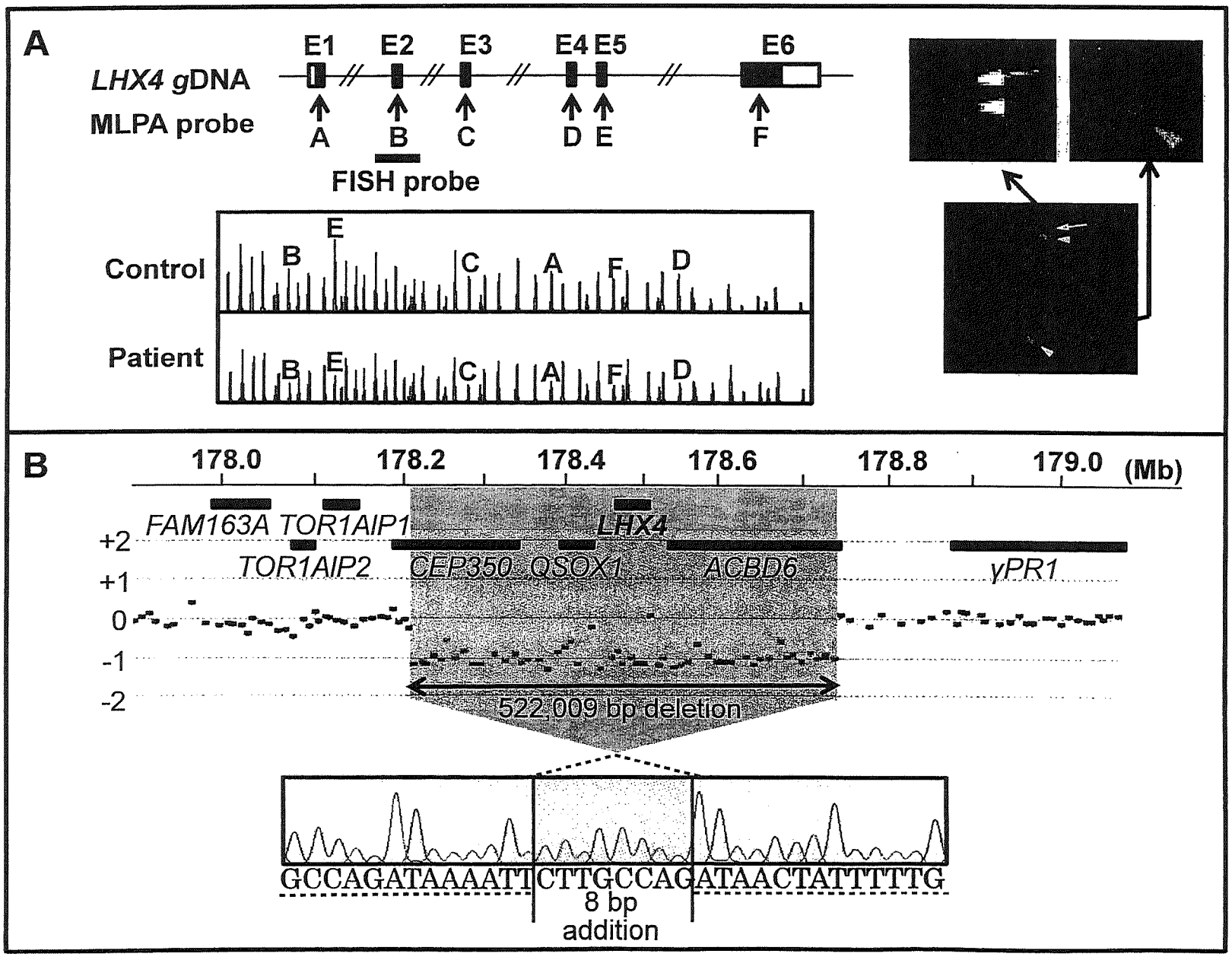
A
LHX4 gDNA
MLPA probe
E1
E2
E3
E4
E5
E6
A
B
C
D
E
F
FISH probe
Control
Patient
B
178.0
178.2
178.4
178.6
178.8
179.0
(Mb)
FAM163A
TOR1AIP1
TOR1AIP2
CEP350
QSOX1
LHX4
ACBD6
γPR1
+2
+1
0
-1
-2
522,009 bp deletion
GCCAGATAAAATTCTTGCCAGATAACTATTTTTG
8 bp
addition

The IG-DMR and the *MEG3*-DMR at Human Chromosome 14q32.2: Hierarchical Interaction and Distinct Functional Properties as Imprinting Control Centers

Masayo Kagami[1], Maureen J O'Sullivan[2], Andrew J Green[3], Yoshiyuki Watabe[4], Osamu Arisaka[4], Nobuhide Masawa[5], Kentarou Matsuoka[6], Maki Fukami[1], Keiko Matsubara[1], Fumiko Kato[1], Anne C Ferguson-Smith[7], and Tsutomu Ogata[1]*

1 Department of Endocrinology and Metabolism, National Research Institute for Child Health and Development, Tokyo, Japan, **2** Department of Pathology, Our Lady's Children's Hospital, and School of Medicine, Trinity College, Dublin, Ireland, **3** National Center for Medical Genetics, University College Dublin, Our Lady's Hospital, and School of Medicine and Medical Science, University College, Dublin, Ireland, **4** Department of Pediatrics, Dokkyo University School of Medicine, Tochigi, Japan, **5** Department of Pathology, Dokkyo University School of Medicine, Tochigi, Japan, **6** Department of Pathology, National Center for Child Health and Development, Tokyo, Japan, **7** Department of Physiology, Development and Neuroscience, University of Cambridge, Cambridge, UK.

Running head: Imprinting Control Centers at Human 14q32.2

*Correspondence: tomogata@nch.go.jp.

Abstract

Human chromosome 14q32.2 harbors the germline-derived primary *DLK1-MEG3* intergenic differentially methylated region (IG-DMR) and the postfertilization-derived secondary *MEG3*-DMR, together with multiple imprinted genes. Although previous studies in cases with microdeletions and epimutations affecting both DMRs and paternal/maternal uniparental disomy 14 (upd(14)pat/mat)-like phenotypes argue for a critical regulatory function of the two DMRs for the 14q32.2 imprinted region, the precise role of individual DMR remains to be clarified. We studied an infant with upd(14)pat body and placental phenotypes (patient 1) and the mother with upd(14)mat-like body phenotype (patient 2), and a neonate with upd(14)pat body, but no placental, phenotype (patient 3). Structural analysis showed a familial 8,558 bp microdeletion involving the IG-DMR alone in patients 1 and 2, and a *de novo* 4,303 bp microdeletion involving the *MEG3*-DMR alone in patient 3. Methylation and expression analyses revealed that loss of the hypomethylated IG-DMR of maternal origin in patient 1 was associated with epimutation (hypermethylation) of the *MEG3*-DMR in the body and caused paternalization of the imprinted region in examined body and placental tissues, whereas loss of the hypomethylated *MEG3*-DMR of maternal origin in patient 3 permitted normal methylation pattern of the IG-DMR and resulted in maternal to paternal epigenotypic alteration in examined body tissues. The imprinting status appeared normal in patient 2. These results, together with the finding that the IG-DMR remains as a DMR and the *MEG3*-DMR exhibits a non-DMR in the placenta, imply that the IG-DMR and the *MEG3*-DMR function as imprinting control centers in the placenta and the body, respectively, with a hierarchical interaction for the methylation pattern in the body. In addition, the phenotype of patient 2 may suggest the presence of a *cis*-acting regulatory element for *DLK1* expression around the IG-DMR.

Author Summary

Human chromosome 14q32.2 imprinted region harbors the germline-derived primary *DLK1-MEG3* intergenic differentially methylated region (IG-DMR) and the postfertilization-derived secondary *MEG3*-DMR, together with multiple imprinted genes. Consistent with this, paternal and maternal uniparental disomy 14 (upd(14)pat and upd(14)mat) causes distinct phenotypes. Here, we show that the IG-DMR acts as an upstream regulator for the methylation pattern of the *MEG3*-DMR in the body but not in the placenta, and that the IG-DMR and the *MEG3*-DMR function as imprinting control centers in the placenta and the body, respectively. To our knowledge, this is the first study demonstrating not only different roles between the primary and the secondary DMRs at a single imprinted region, but also an essential regulatory function for the secondary DMR. Thus, the results provide significant advance in the clarification of underlying mechanisms involved in the imprinting regulation at the 14q32.2 region and the development of upd(14)pat/mat phenotype. In addition, we also suggest the presence of a *cis*-acting regulatory element for the *DLK1* expression around the IG-DMR.

Introduction

Human chromosome 14q32.2 carries a cluster of protein-coding paternally expressed genes (*PEGs*) such as *DLK1* and *RTL1* and non-coding maternally expressed genes (*MEGs*) such as *MEG3* (alias, *GTL2*), *RTL1as* (*RTL1* antisense), *MEG8*, *snoRNAs*, and *microRNAs* [1,2]. Consistent with this, paternal uniparental disomy 14 (upd(14)pat) results in a unique phenotype characterized by facial abnormality, small bell-shaped thorax, abdominal wall defects, placentomegaly, and polyhydramnios [2,3], and maternal uniparental disomy 14 (upd(14)mat) leads to less-characteristic but clinically discernible features including growth failure [2,4].

The 14q32.2 imprinted region also harbors two differentially methylated regions (DMRs), i.e., the germline-derived primary *DLK1-MEG3* intergenic DMR (IG-DMR) and the postfertilization-derived secondary *MEG3*-DMR [1,2]. Both DMRs are hypermethylated after paternal transmission and hypomethylated after maternal transmission in the body, whereas in the placenta the IG-DMR alone remains as a DMR and the *MEG3*-DMR is rather hypomethylated [1,2]. Furthermore, previous studies in cases with upd(14)pat/mat-like phenotypes have revealed that epimutations (hypermethylation) and microdeletions affecting both DMRs of maternal origin cause paternalization of the 14q32.2 imprinted region, and that epimutations (hypomethylation) affecting both DMRs of paternal origin cause maternalization of the 14q32.2 imprinted region, while microdeletions involving the DMRs of paternal origin have no effect on the imprinting status [2,5–8]. These findings, together with the notion that parent-of-origin specific expression patterns of imprinted genes are primarily dependent on the methylation status of the DMRs [9], argue for a critical regulatory function of the two DMRs for the 14q32.2 imprinted region, with possible different effects between the body and the placenta.

However, the precise role of individual DMR remains to be clarified. Here, we report that the IG-DMR and the *MEG3*-DMR show a hierarchical interaction for the methylation pattern in the body, and function as imprinting control centers in the placenta and the body, respectively. To our knowledge, this is the first study demonstrating not only different roles between the primary and secondary DMRs at a single imprinted region, but also an essential regulatory function for the secondary DMR.

Results

Clinical reports

We identified familial cases, a proband (patient 1) and the mother (patient 2), and a sporadic case (patient 3) Detailed phenotypes of patients 1 and 3 are summarized in Table 1 (see also Figure 1), and those of patient 2 are summarized in Table 2. In brief, patient 1 was delivered by a caesarean section at 33 weeks of gestation due to progressive polyhydramnios despite amnioreduction at 28 and 30 weeks of gestation, whereas patient 3 was born at 28 weeks of gestation by a vaginal delivery due to progressive labor without discernible polyhydramnios. Placentomegaly was observed in patient 1 but not in patient 3. Patients 1 and 3 were found to have characteristic face, small bell-shaped thorax with coat hanger appearance of the ribs, and omphalocele. Patient 1 received surgical treatment for omphalocele immediately after birth and mechanical ventilation for several months. At present, she is 5.5 months of age, and still requires intensive care including oxygen administration and tube feeding. Patient 3 died at four days of age due to massive intracranial hemorrhage, while receiving intensive care including mechanical ventilation. Thus, upd(14)pat body phenotype was unequivocally exhibited by patients 1 and 3, whereas upd(14)pat placental phenotype, which has invariably been identified by 28 weeks of gestation in upd(14)pat patients [2,3], was present in patient 1 and absent from patient 3. Patient 2 was noticed to have upd(14)mat-like body phenotype including short stature, obesity, and small hands, through familial studies. The father of patient 1 and the parents of patient 3 were clinically normal.

Sample preparation

We isolated genomic DNA (gDNA) and transcripts (*mRNAs*, *snoRNAs*, and *microRNAs*) from fresh leukocytes of patients 1 and 2, the father of patient 1, and the parents of patient 3, from fresh skin fibroblasts of patient 3, and from formalin-fixed and paraffin-embedded placental samples of patient 1 and similarly treated pituitary and adrenal samples of patient 3 (although multiple body tissues were available in patient 3, useful gDNA and transcript samples were not obtained from other tissues probably due to drastic post-mortem degradation). We also made metaphase spreads from leukocytes and skin fibroblasts. For comparison, we obtained

control samples from fresh normal adult leukocytes, neonatal skin fibroblasts, and placenta at 38 weeks of gestation, and from fresh leukocytes of upd(14)pat/mat patients and formalin-fixed and paraffin-embedded placenta of a upd(14)pat patient [2,3].

Structural analysis of the imprinted region

We first examined the structure of the 14q32.2 imprinted region (Figure 2). Upd(14) was excluded in patients 1–3 by microsatellite analysis (Table S1), and FISH analysis for the two DMRs identified a familial heterozygous deletion encompassing the IG-DMR alone in patients 1 and 2 and a *de novo* heterozygous deletion encompassing the *MEG3*-DMR alone in patient 3 (Figure 2). The microdeletions were further localized by SNP genotyping for 66 loci (Table S1) and quantitative real-time PCR (q-PCR) analysis for four regions around the DMRs (Figure S1A), and serial direct sequencing for the long PCR products harboring the deletion junctions successfully identified the fusion points of the microdeletions in patients 1–3 (Figure 2). According to the NT_026437 sequence data at the NCBI Database (Genome Build 36.3) (http://preview.ncbi.nlm.nih.gov/guide/), the deletion size was 8,558 bp (82,270,449–82,279,006 bp) for the microdeletion in patients 1 and 2, and 4,303 bp (82,290,978–82,295,280 bp) for the microdeletion in patient 3. The microdeletion in patient 3 also involved the 5' part of *MEG3* and five of the seven putative CTCF binding sites A–G [13], and was accompanied by insertion of a 66 bp sequence duplicated from *MEG3* intron 5 (82,299,727–82,299,792 bp on NT_026437). Direct sequencing of the exonic or transcribed regions detected no mutation in *DLK1*, *MEG3*, and *RTL1*, although several cDNA polymorphisms (cSNPs) were identified (Table S1). Oligoarray comparative genomic hybridization identified no other discernible structural abnormality (Figure S1B).

Methylation analysis of the two DMRs

We next studied methylation patterns of the previously reported IG-DMR (CG4 and CG6) and the *MEG3*-DMR (CG7) [2] and those of the seven putative CTCF binding sites, using bisulfite treated gDNA samples (Figure 3A). Bisulfite sequencing and combined bisulfite restriction analysis using body samples revealed a hypermethylated IG-DMR and *MEG3*-DMR

in patient 1, a hypomethylated IG-DMR and differentially methylated *MEG3*-DMR in patient 2, and a differentially methylated IG-DMR and hypermethylated *MEG3*-DMR in patient 3, and bisulfite sequencing using placental samples showed a hypermethylated IG-DMR and rather hypomethylated *MEG3*-DMR in patient 1 (Figure 3B). Furthermore, bisulfite sequencing revealed that, of the seven putative CTCF binding sites, sites C and D exhibited methylation patterns comparable to those of CG7 (Figure 3C).

Expression analysis of the imprinted genes

Finally, we performed expression analyses, using standard reverse transcriptase (RT)-PCR and/or q-PCR analysis for multiple imprinted genes in this region (Figure 4A–C). For leukocytes, weak expression was detected for *MEG3* and *SNORD114-29* in a control subject and patient 2 but not in patient 1. For skin fibroblasts, although all *MEGs* but no *PEGs* were expressed in control subjects, neither *MEGs* nor *PEGs* were expressed in patient 3. For placentas, although all imprinted genes were expressed in control subjects, *PEGs* only were expressed in patient 1. For the pituitary and adrenal of patient 3, *DLK1* expression alone was identified.

Expression pattern analyses using informative cSNPs revealed monoallelic *MEG3* expression in the leukocytes of patient 2 (Figure 4D), and biparental *RTL1* expression in the placenta of patient 1 (no informative cSNP was detected for *DLK1*) and biparental *DLK1* expression in the pituitary and adrenal of patient 3 (*RTL1* was not expressed in the pituitary and adrenal) (Figure 4E), as well as maternal *MEG3* expression in the control leukocytes and paternal *RTL1* expression in the control placentas (Figure S2). Although we also attempted q-PCR analysis, precise assessment was impossible for *MEG3* in patient 2 because of faint expression level in leukocytes and for *RTL1* in patient 1 and *DLK1* in patient 3 because of poor quality of mRNAs obtained from formalin-fixed and paraffin-embedded tissues.

Discussion

The data of the present study are summarized in Figure 5. Parental origin of the microdeletion positive chromosomes is based on the methylation patterns of the preserved

DMRs in patients 1–3 as well as maternal transmission in patient 1. Loss of the hypomethylated IG-DMR of maternal origin in patient 1 was associated with epimutation (hypermethylation) of the *MEG3*-DMR in the body and caused paternalization of the imprinted region and typical upd(14)pat body and placental phenotypes, whereas loss of the hypomethylated *MEG3*-DMR of maternal origin in patient 3 permitted normal methylation pattern of the IG-DMR in the body and resulted in maternal to paternal epigenotypic alteration and typical upd(14)pat body, but no placental, phenotype. In this regard, while a 66 bp segment was inserted in patient 3, this segment contains no known regulatory sequence [14] or evolutionarily conserved element [15] (also examined with a VISTA program, http://genome.lbl.gov/vista/index.shtml). Similarly, while no control samples were available for pituitary and adrenal, the previous study in human subjects has shown paternal *DLK1* expression in adrenal as well as monoallelic *DLK1* and *MEG3* expressions in various tissues [14]. Furthermore, the present and the previous studies [2] indicate that this region is imprinted in the placenta as well as in the body. Thus, these results, in conjunction with the finding that the IG-DMR remains as a DMR and the *MEG3*-DMR exhibits a non-DMR in the placenta [2], imply the following: (1) the IG-DMR functions hierarchically as an upstream regulator for the methylation pattern of the *MEG3*-DMR on the maternally inherited chromosome in the body, but not in the placenta; (2) the hypomethylated *MEG3*-DMR functions as an essential imprinting regulator for both *PEGs* and *MEGs* in the body; and (3) in the placenta, the hypomethylated IG-DMR directly controls the imprinting pattern of both *PEGs* and *MEGs*. These notions also explain the epigenotypic alteration in the previous cases with epimutations or microdeletions affecting both DMRs (Figure S3).

For the *MEG3*-DMR, the CTCF binding sites C and D may play a pivotal role in the imprinting regulation. The methylation analysis indicates that the two cites reside within the *MEG3*-DMR, and it is known that the CTCF protein with versatile functions preferentially binds to unmethylated target sequences including the sites C and D [13,16–18]. In this regard, all the *MEGs* in this imprinted region can be transcribed together in the same orientation and show a strikingly similar tissue expressions pattern [1,15], whereas *PEGs* are transcribed in different directions and are co-expressed with *MEGs* only in limited cell-types [1,19]. It is possible, therefore, that preferential CTCF binding to the grossly unmethylated sites C and D

activates all the *MEGs* as a large transcription unit and represses all the *PEGs* perhaps by influencing chromatin structure and histone modification independently of the effects of expressed *MEGs*. In support of this, CTCF protein acts as a transcriptional activator for *Gtl2* (the mouse homolog for *MEG3*) in the mouse [20].

Patient 2 had upd(14)mat-like body phenotype. This may be co-incidental, because her clinical features are not specific to upd(14)mat. Indeed, consistent with the notion that loss of the paternally derived IG-DMR does not affect the imprinted status [2,21], *MEG3* showed normal monoallelic expression in the presence of the differentially methylated *MEG3*-DMR. However, since upd(14)mat phenotype is primarily ascribed to loss of functional *DLK1* with an additional effect of loss of functional *RTL1* (Figure S3B) [2,22,23], the microdeletion involving the IG-DMR may have affected a *cis*-acting regulatory element for *DLK1* expression (Figure 5). In this case, the microdeletion is predicted to affect *DLK1* expression on the paternalized chromosome of maternal origin in patient 1. However, this is not inconsistent with the typical upd(14)pat phenotype in patient 1, because patient 1 had clear biparental *RTL1* expression in the absence of *MEGs* expression. Indeed, typical upd(14)pat body and placental phenotype has primarily been ascribed to markedly elevated *RTL1* expression, which is explained by the synergic effect of two active copies of *RTL1* and the absence of functional *RTL1as* as a repressor for *RTL1* [21,23–25], rather than to doubled *DLK1* expression (Figure S3A) [2].

This imprinted region has also been studied in the mouse. Clinical and molecular findings in wildtype mice [1,26,27], mice with PatDi(12) (paternal disomy for chromosome 12 harboring this imprinted region) [28–30], and mice with targeted deletions for the IG-DMR (ΔIG-DMR) [21,26] and for the *Gtl2*-DMR (the mouse homolog for the *MEG3*-DMR) (Δ*Gtl2*-DMR) [31] are summarized in Table 3. These data, together with human data, provide several informative findings. First, in both the human and the mouse, the IG-DMR is differentially methylated in both the body and the placenta, whereas the *MEG3*/*Gtl2*-DMR is differentially methylated in the body and exhibits non-DMR in the placenta. Second, the IG-DMR and the *MEG3*/*Gtl2*-DMR show a hierarchical interaction on the maternally derived chromosome in both the human and the mouse bodies. Indeed, the *MEG3*/*Gtl2*-DMR is epimutated in patient 1 and mice with maternally inherited ΔIG-DMR, and the IG-DMR is

normally methylated in patient 3 and mice with maternally inherited Δ*Gtl2*-DMR. Third, the function of the IG-DMR is comparable between human and mouse bodies and different between human and mouse placentas. Indeed, patient 1 has upd(14)pat body and placental phenotypes, whereas mice with the ΔIG-DMR of maternal origin have PatDi(12)-compatible body phenotype and apparently normal placental phenotype. It is likely that imprinting regulation in the mouse placenta is contributed by some mechanism(s) other than the methylation pattern of the IG-DMR, such as chromatin conformation [26,32,33].

Unfortunately, however, the data of Δ*Gtl2*-DMR mice appears to be drastically complicated by the retained neomycin cassette in the upstream region of *Gtl2*. Indeed, it has been shown that the insertion of a *lacZ* gene or a neomycin gene in the similar upstream region of *Gtl2* causes severely dysregulated expression patterns and abnormal phenotypes after both paternal and maternal transmissions [34,35], and that deletion of the inserted neomycin gene results in apparently normal expression patterns and phenotypes after both paternal and maternal transmissions [35]. (In this regard, although a possible influence of the inserted 66 bp segment can not be excluded formally in patient 3, phenotype and expression data in patient 3 are compatible with simple paternalization of the imprinted region.) In addition, since the apparently normal phenotype in mice homozygous for Δ*Gtl2*-DMR is reminiscent of that in sheep homozygous for the callipyge mutation [36], a complicated mechanism(s) such as the polar overdominance may be operating in the Δ*Gtl2*-DMR mice [37]. Thus, it remains to be clarified whether the *MEG3/Gtl2*-DMR has a similar or different function between the human and the mouse.

In summary, the results show a hierarchical interaction and distinct functional properties of the IG-DMR and the *MEG3*-DMR in imprinting control. Thus, this study provides significant advance in the clarification of underlying mechanisms involved in the imprinting regulation at the 14q32.2 imprinted region and the development of upd(14)pat/mat phenotype.

Methods

Ethics Statement

This study was approved by the Institutional Review Board Committees at National Center for Child health and Development, University College Dublin, and Dokkyo University School of Medicine, and performed after obtaining written informed consent.

Primers

All the primers utilized in this study are summarized in Table S2.

Sample preparation

For leukocytes and skin fibroblasts, genomic DNA (gDNA) samples were extracted with FlexiGene DNA Kit (Qiagen), and RNA samples were prepared with RNeasy Plus Mini (Qiagen) for *DLK1, MEG3, RTL1*, *MEG8* and *snoRNAs*, and with mirVana^{TM} miRNA Isolation Kit (Ambion) for *microRNAs*. For paraffin-embedded tissues including the placenta, brain, lung, heart, liver, spleen, kidney, bladder, and small intestine, gDNA and RNA samples were extracted with RecoverAll^{TM} Total Nucleic Acids Isolation Kit (Ambion) using slices of 40 μm thick. For fresh control placental samples, gDNA and RNA were extracted using ISOGEN (Nippon Gene). After treating total RNA samples with DNase, cDNA samples for *DLK1, MEG3, MEG8*, and *snoRNAs* were prepared with oligo(dT) primers from 1 μg of RNA using Superscript III Reverse Transcriptase (Invitrogen), and those for *microRNAs* were synthesized from 300 ng of RNA using TaqMan MicroRNA Reverse Transcription Kit (Applied Biosystems). For *RTL1*, cDNA samples were synthesized with *RTL1*-specific primers that do not amplify *RTL1as*. Control gDNA and cDNA samples were extracted from adult leukocytes and neonatal skin fibroblasts purchased from Takara Bio Inc. Japan, and from a fresh placenta of 38 weeks of gestation. Metaphase spreads were prepared from leukocytes and skin fibroblasts using colcemide (Invitrogen).

Structural analysis

Microsatellite analysis and SNP genotyping were performed as described previously [2].

For FISH analysis, metaphase spreads were hybridized with a 5,104 bp FISH-1 probe and a 5,182 bp FISH-2 probe produced by long PCR, together with an RP11-566I2 probe for 14q12 used as an internal control [2]. The FISH-1 and FISH-2 probes were labeled with digoxigenin and detected by rhodamine anti-digoxigenin, and the RP11-566I2 probe was labeled with biotin and detected by avidin conjugated to fluorescein isothiocyanate. For quantitative real-time PCR analysis, the relative copy number to RNaseP (catalog No: 4316831, Applied Biosystems) was determined by the Taqman real-time PCR method using the probe-primer mix on an ABI PRISM 7000 (Applied Biosystems). To determine the breakpoints of microdeletions, sequence analysis was performed for long PCR products harboring the fusion points, using serial forward primers on the CEQ 8000 autosequencer (Beckman Coulter). Direct sequencing was also performed on the CEQ 8000 autosequencer. Oligoarray comparative genomic hybridization was performed with 1x244K Human Genome Array (catalog No: G4411B) (Agilent Technologies), according to the manufacturer's protocol.

Methylation analysis

Methylation analysis was performed for gDNA treated with bisulfite using the EZ DNA Methylation Kit (Zymo Research). After PCR amplification using primer sets that hybridize both methylated and unmethylated clones because of lack of CpG dinucleotides within the primer sequences, the PCR products were digested with appropriate restriction enzymes for combined bisulfite restriction analysis. For bisulfite sequencing, the PCR products were subcloned with TOPO TA Cloning Kit (Invitrogen) and subjected to direct sequencing on the CEQ 8000 autosequencer.

Expression analysis

Standard RT-PCR was performed for *DLK1*, *RTL1*, *MEG3*, *MEG8*, and *snoRNAs* using primers hybridizing to exonic or transcribed sequences, and one μl of PCR reaction solutions was loaded onto Gel-Dye Mix (Agilent). Taqman real-time PCR was carried out using the probe-primer mixtures (assay No: Hs00292028 for *MEG3* and Hs00419701 for *MEG8*; assay ID: 001028 for *miR433*, 000452 for *miR127*, 000568 for *miR379*, and 000477 for *miR154*) on

the ABI PRISM 7000. Data were normalized against *GAPDH* (catalog No: 4326317E) for *MEG3* and *MEG8* and against *RNU48* (assay ID: 0010006) for the remaining *miRs*. The expression studies were performed three times for each sample.

To examine the imprinting status of *MEG3* in the leukocytes of patient 2, direct sequence data for informative cSNPs were compared between gDNA and cDNA. To analyze the imprinting status of *RTL1* in the placental sample of patient 1 and that of *DLK1* in the pituitary and adrenal samples of patient 3, RT-PCR products containing exonic cSNPs informative for the parental origin were subcloned with TOPO TA Cloning Kit, and multiple clones were subjected to direct sequencing on the CEQ 8000 autosequencer. Furthermore, *MEG3* expression pattern was examined using leukocyte gDNA and cDNA samples from multiple normal subjects and leukocyte gDNA samples from their mothers, and *RTL1* expression pattern was analyzed using gDNA and cDNA samples from multiple fresh normal placentas and leukocyte gDNA from the mothers.

Acknowledgments

This work was supported by grants from the Ministry of Health, Labor, and Welfare, from the Ministry of Education, Science, Sports and Culture, and from Takeda Science Foundation.

Author Contributions

Conceived and designed the experiments: MK ACF-S TO. Performed the experiments: MK MF KM FK. Contributed reagents/materials/analysis tool: MJO AJG YW OA NM KM TO. Wrote the paper: TO.

Competing Interests

The authors have declared that no competing interests exist.